Supporting Information (SI)

Thermomechanical Properties of Solid "Liquid Crystalline" Films from Hot-Pressed Synthetic Polypeptides of Various Macromolecular Architectures

Stephen R. Ekatan[1], Tianrui Xue[5], Ziyuan Song[4], Tianjian Yang[1], Dennis Ndaya[1], Montgomery T. Shaw[1,3], Jianjun Cheng[4,5*], and Yao Lin[1,2*]*

[1]Polymer Program, Institute of Materials Science, University of Connecticut, Storrs, CT 06269, USA. [2]Department of Chemistry, University of Connecticut, Storrs, CT 06269, USA. [3]Department of Chemical & Biomolecular Engineering, University of Connecticut, Storrs, CT 06269, USA. [4]Department of Materials Science and Engineering, University of Illinois at Urbana-Champaign, Urbana, IL 61801, USA. [5]Department of Chemistry, University of Illinois at Urbana-Champaign, Urbana, IL 61801, USA.

***Email: yao.lin@uconn.edu; jianjunc@illinois.edu; montgomery.shaw@uconn.edu**

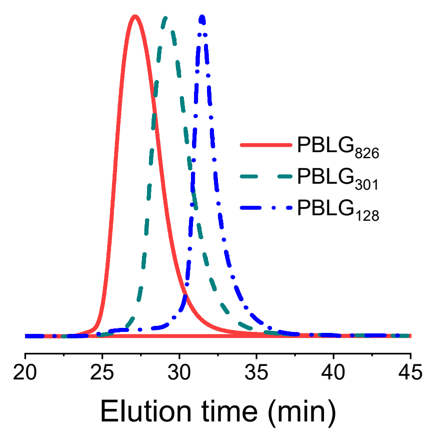

Figure S1. Normalized GPC-LS traces of linear PBLG of three different chain length. GPC characterization results: $PBLG_{128}$, M_n = 28 kDa, $Đ$ = 1.25; $PBLG_{301}$, M_n = 66 kDa, $Đ$ = 1.31; $PBLG_{826}$, M_n = 181 kDa, $Đ$ = 1.32.

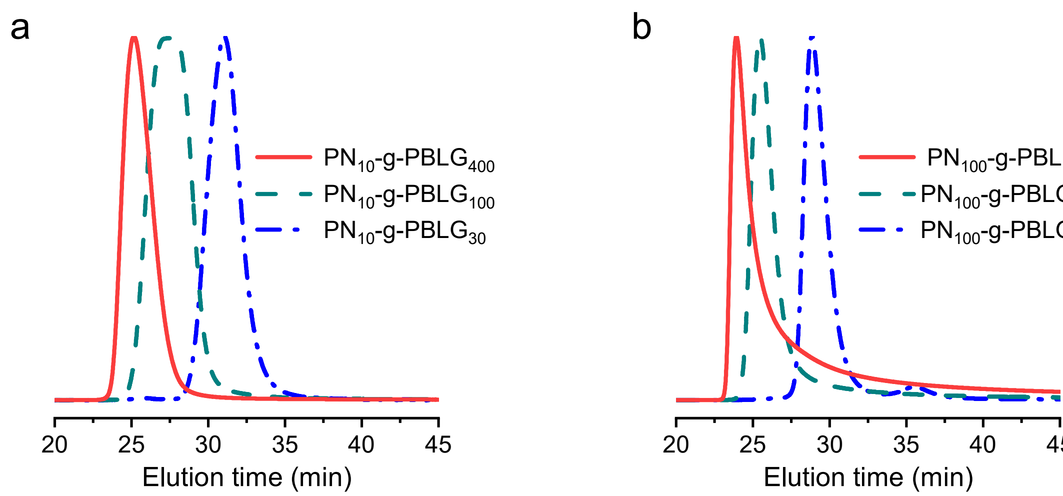

Figure S2. Normalized GPC-LS traces of comb-like and brush-like macromolecules. (a) comb-like. (b) brush-like. The high designed MWs of PN_{100}-*g*-$PBLG_{400}$ induced poor solubility of the brush-like polymers and caused the tailing signal in their GPC traces.

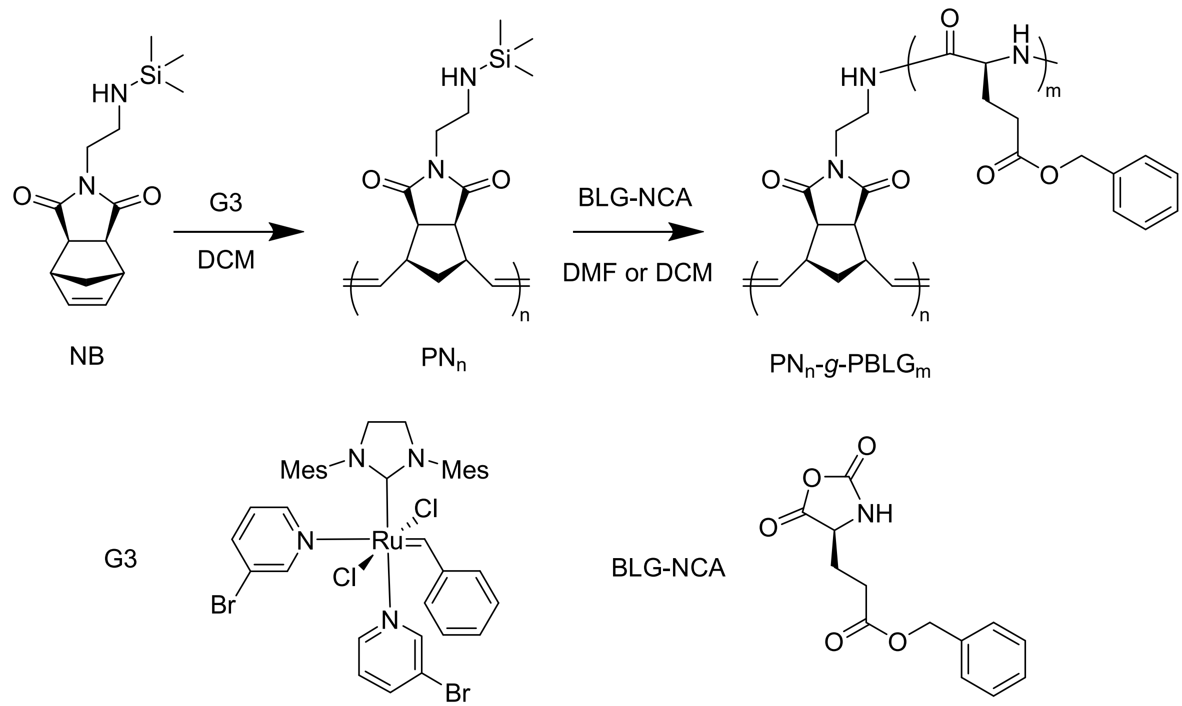

Figure S3. Synthetic route to comb-like and brush-like macromolecules PN$_n$-g-PBLG$_m$.

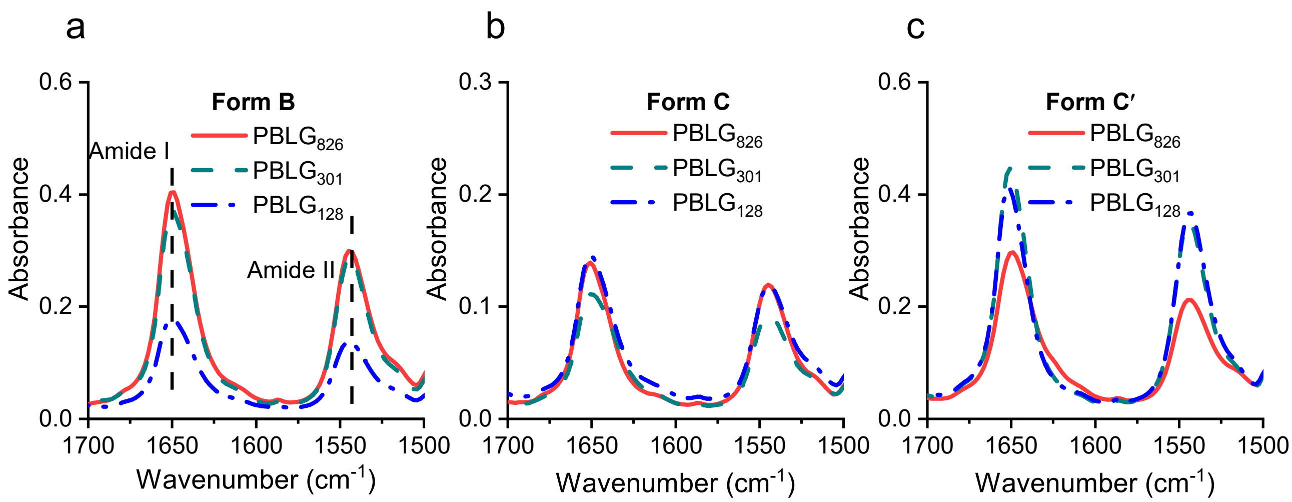

Figure S4. FTIR Spectra of linear PBLG films processed using three different methods showing the α-helical amide I and amide II peaks. (a) cast from DMF. (b) cast from EDC. (c) hot pressed. Linear PBLG with three different chain lengths were processed. Amide 1 peak (~1649 cm^{-1}), Amide II peak (~1545 cm^{-1}).

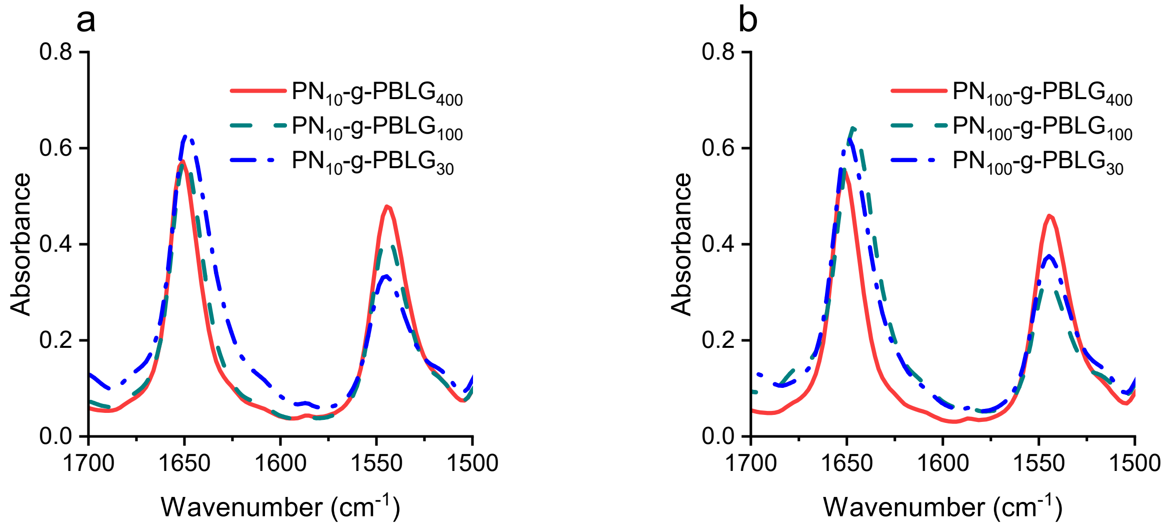

Figure S5. FTIR Spectra of hot pressed films of comb-like and brush-like macromolecules showing the α-helical amide I and amide II peaks. (a) Comb-like. (b) Brush-like. Amide 1 peak (~1649 cm^{-1}), Amide II peak (~1545 cm^{-1}).

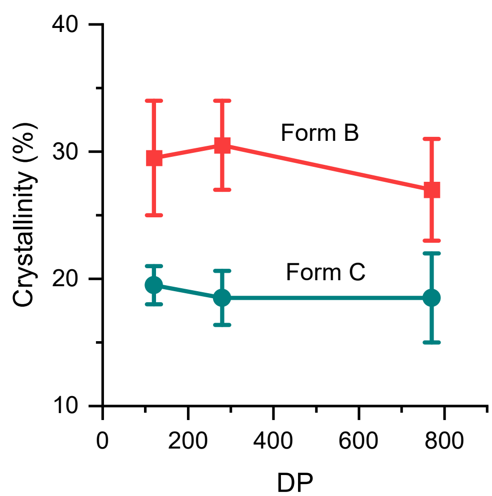

Figure S6. Crystallinity of PBLG cast films with X-ray beam edge-on. The crystallinities are obtained from the X-ray diffraction curves by estimating the area under the crystalline regions and the amorphous hump using Fityk curve fitting and data analysis software. Form B is cast from DMF, Form C is cast from EDC.

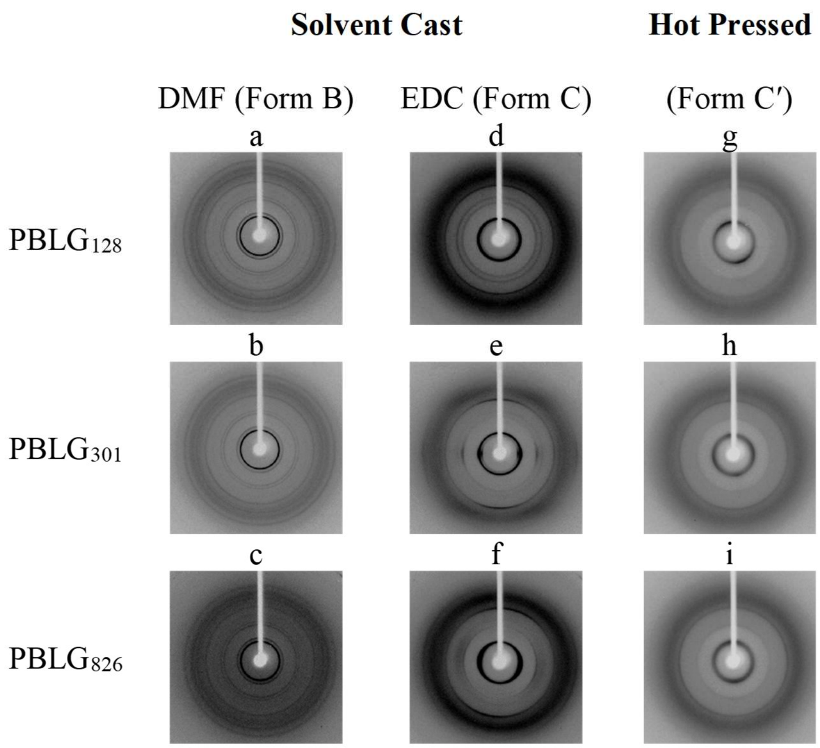

Figure S7. X-ray diffraction patterns of PBLG films of three different chain lengths generated using solvent casting and hot pressing processes. The images were recorded with the film surface normal to the incident X-ray beam (normal view). (a-c) Form B cast from DMF. (d-f) Form C cast from EDC. (g-i) Form C′ processed by hot pressing. X-ray diffraction patterns were obtained with Ni-filtered Cu Kα radiation (40 kV, 10 mA).

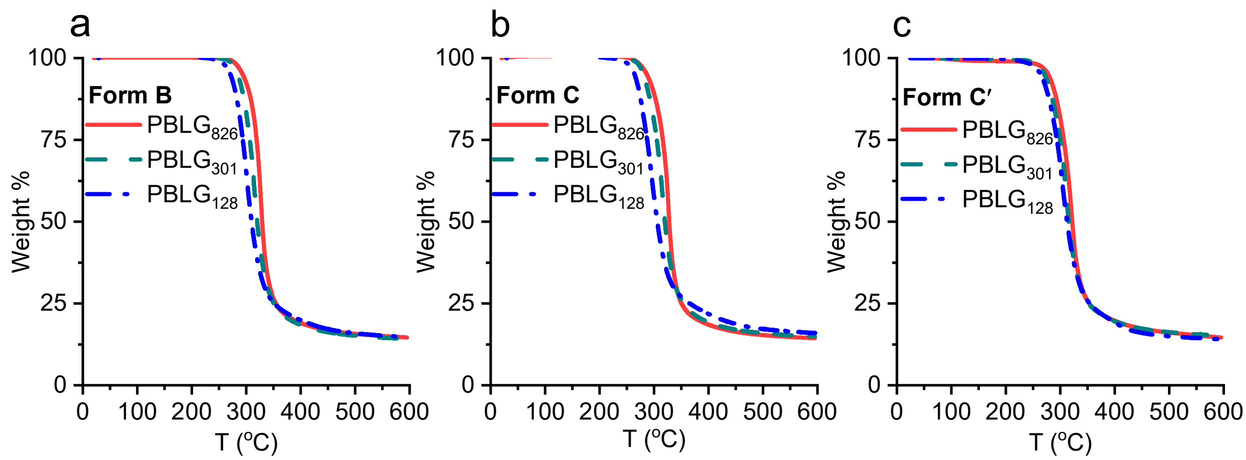

Figure S8. Representative TGA profiles of PBLG films processed by solvent casting and hot pressing showing the weight change with temperature. (a) Form B (cast from DMF). **(**b) Form C (cast from EDC). (c) Form C′ (hot pressed).

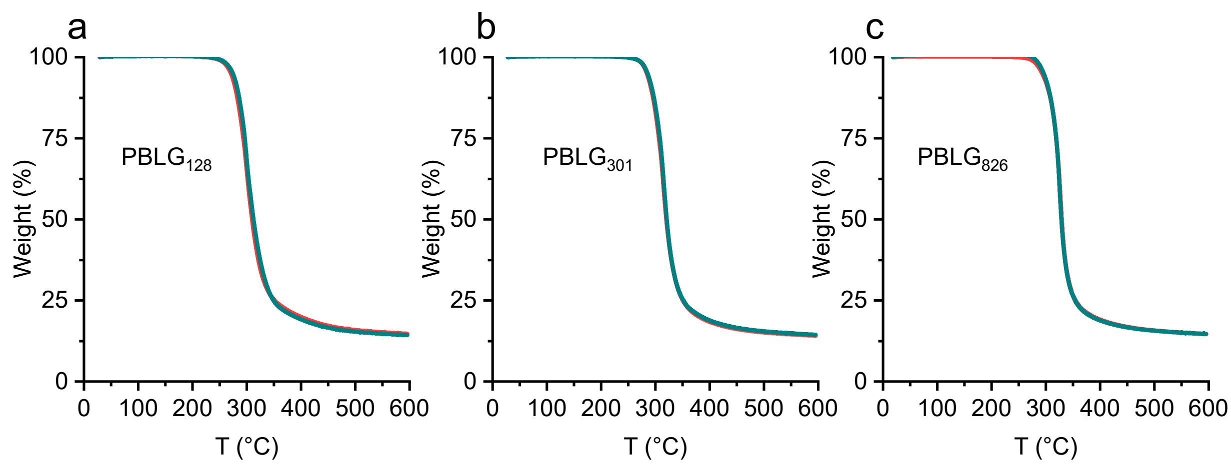

Figure S9. TGA profiles for two replicates of cast films of Form B. (a) $PBLG_{128}$. (b) $PBLG_{301}$. (c) $PBLG_{826}$

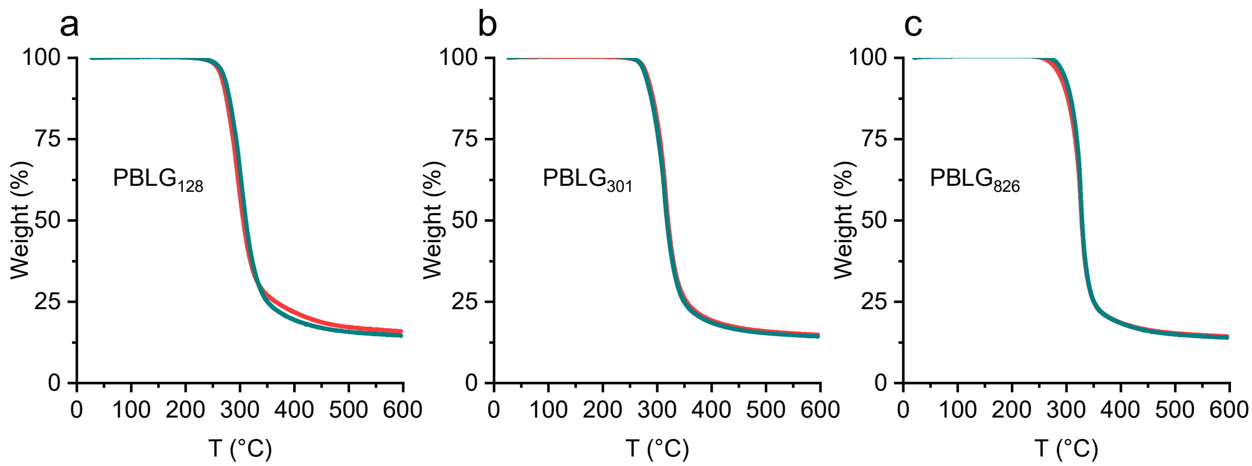

Figure S10. TGA profiles for two replicates of cast films of Form C. (a) $PBLG_{128}$. (b) $PBLG_{301}$. (c) $PBLG_{826}$.

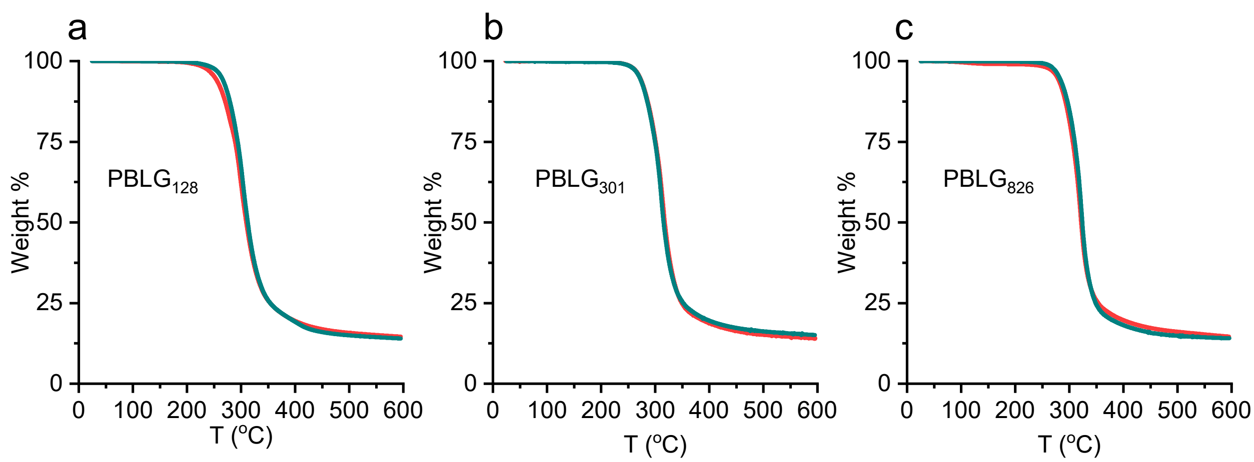

Figure S11. TGA profiles for two replicates of hot pressed films of Form C′. (a) $PBLG_{128}$. (b) $PBLG_{301}$. (c) $PBLG_{826}$.

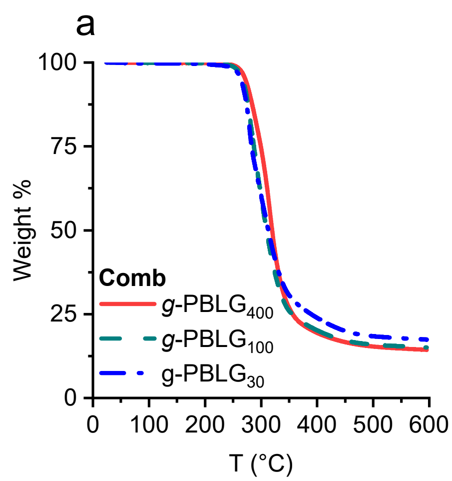

Figure S12. Representative TGA profiles of comb-like and brush-like films showing the weight change with temperature. (a) Comb-like, (b) Brush-like.

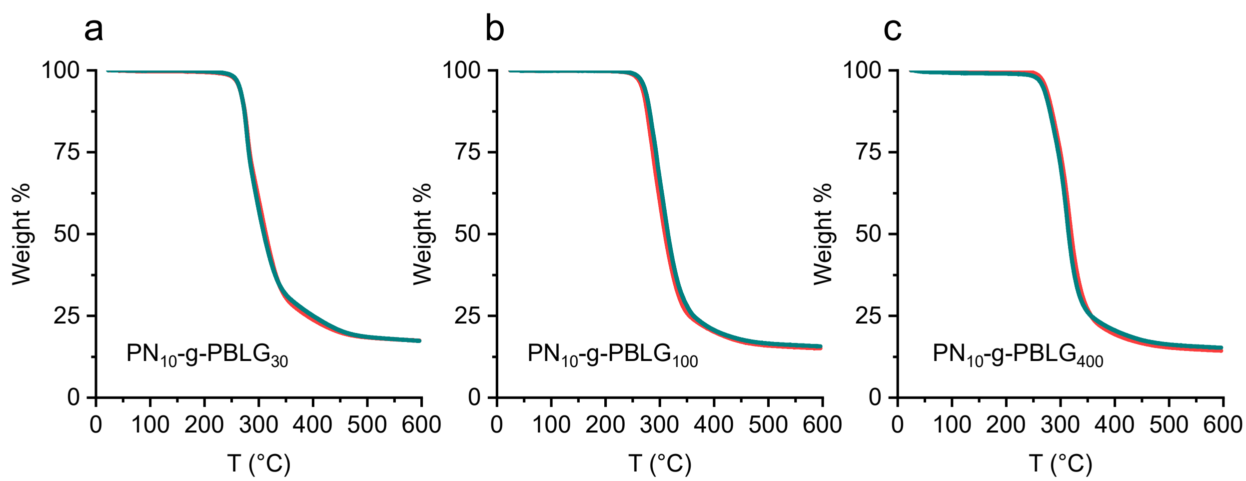

Figure S13. TGA profiles for two replicates of hot pressed films of comb-like macromolecules. (a) PN_{10}-*g*-$PBLG_{30}$. (b) PN_{10}-*g*-$PBLG_{100}$. (c) PN_{10}-*g*-$PBLG_{400}$.

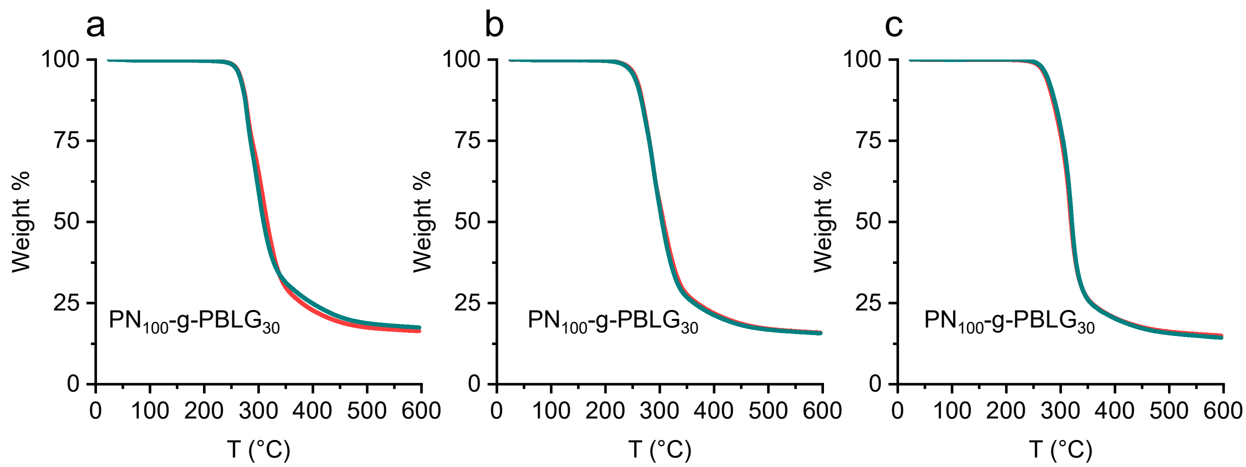

Figure S14. TGA profiles for two replicates of hot pressed films of brush-like macromolecules. (a) PN_{100}-*g*-$PBLG_{30}$. (b) PN_{100}-*g*-$PBLG_{100}$. (c) PN_{100}-*g*-$PBLG_{400}$.

Residual Solvent Effects on Viscoelastic Properties

To probe the effect of residual solvent on viscoelastic properties, compression molded PBLG 66 kDa film were exposed to DMF and EDC solvents and then solvent evaporated at ambient temperature until < 0.5 wt. % of solvent was left based on gravimetric balance measurements. The wt. % was confirmed using TGA analysis. Subsequently, the viscoelastic properties of the respective films were determined using DMA analysis temperature sweep similar to the set up in the Experimental section.

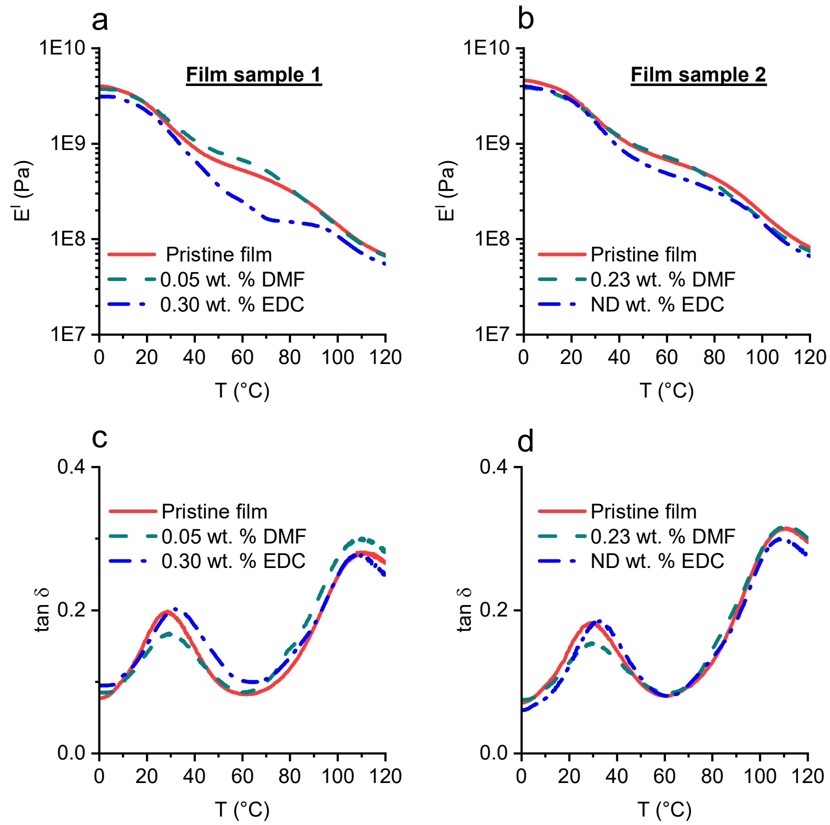

Figure S15. Effect of residual solvent on the viscoelastic properties of PBLG films. (a,b) and (c,d) are tensile storage modulus and tan δ respectively for two replicate samples. There is an appreciable reduction in tensile storage modulus for films exposed to EDC; however, interestingly, films exposed to DMF showed a sustaining of modulus which is in line with the pristine film. These results may suggest that EDC acts as a plasticizer but DMF possibly enhances side-chain interactions the help maintain the modulus as shown.

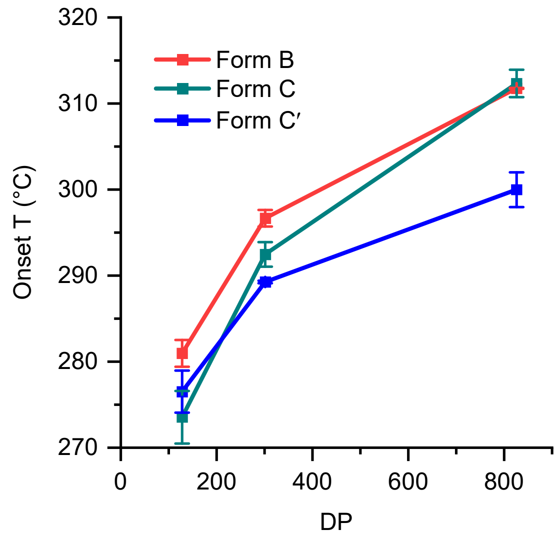

Figure S16. Trend of decomposition onset temperature of films processed from linear PBLG. Results are based on TGA profiles in **Figure S9-S11**.

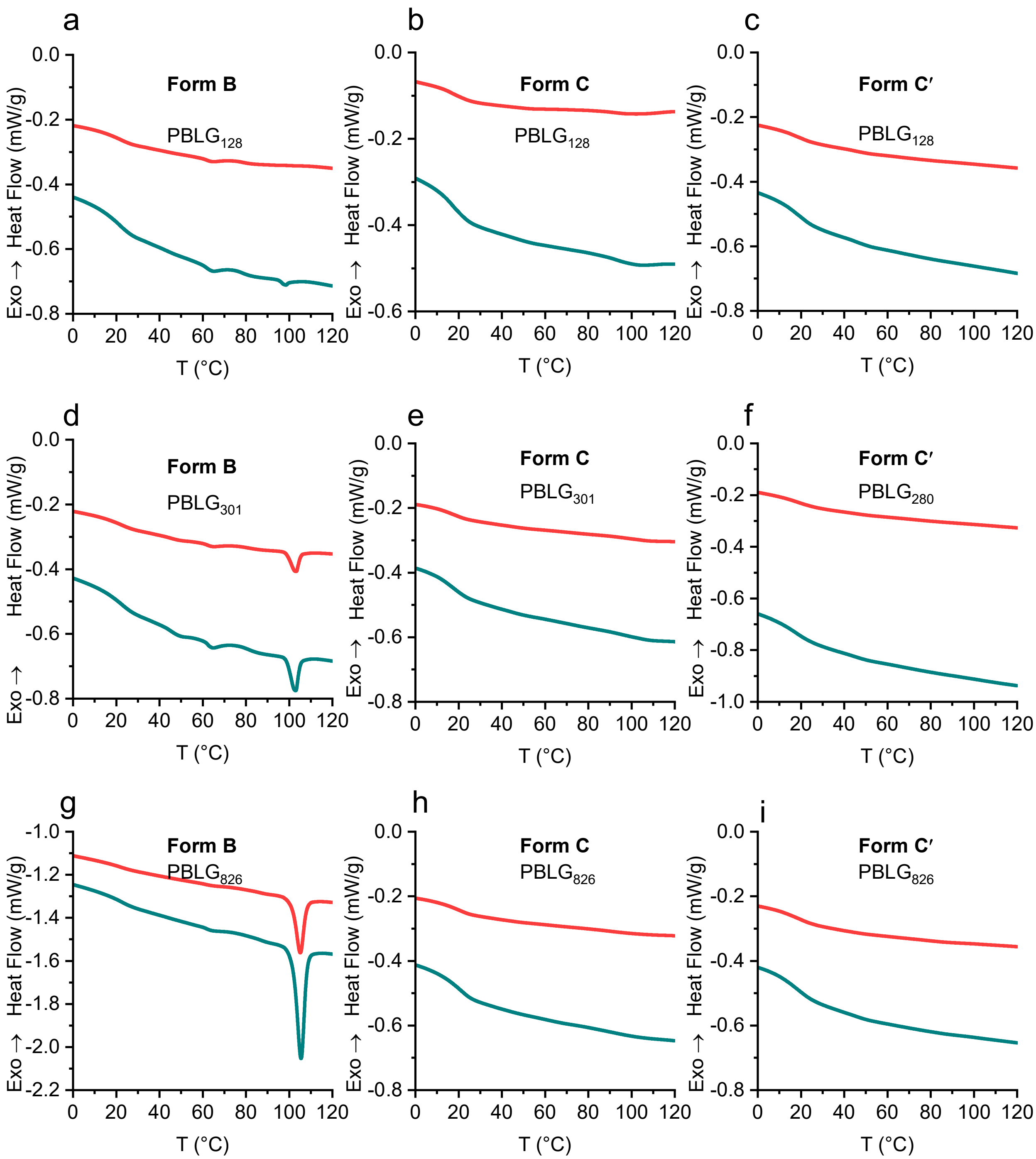

Figure S17. DSC curves on first heating for two replicates of films processed from linear PBLG. (a,d,g) Form B, (b,e,h) Form C, (c,f,i) Form C′. (a-c) $PBLG_{128}$, (d-f) $PBLG_{301}$, (g-i) $PBLG_{826}$. DSC traces in the first heat cycle are affected by the thermal history of the sample under test. Therefore, some observed differences can be attributed to thermal history.

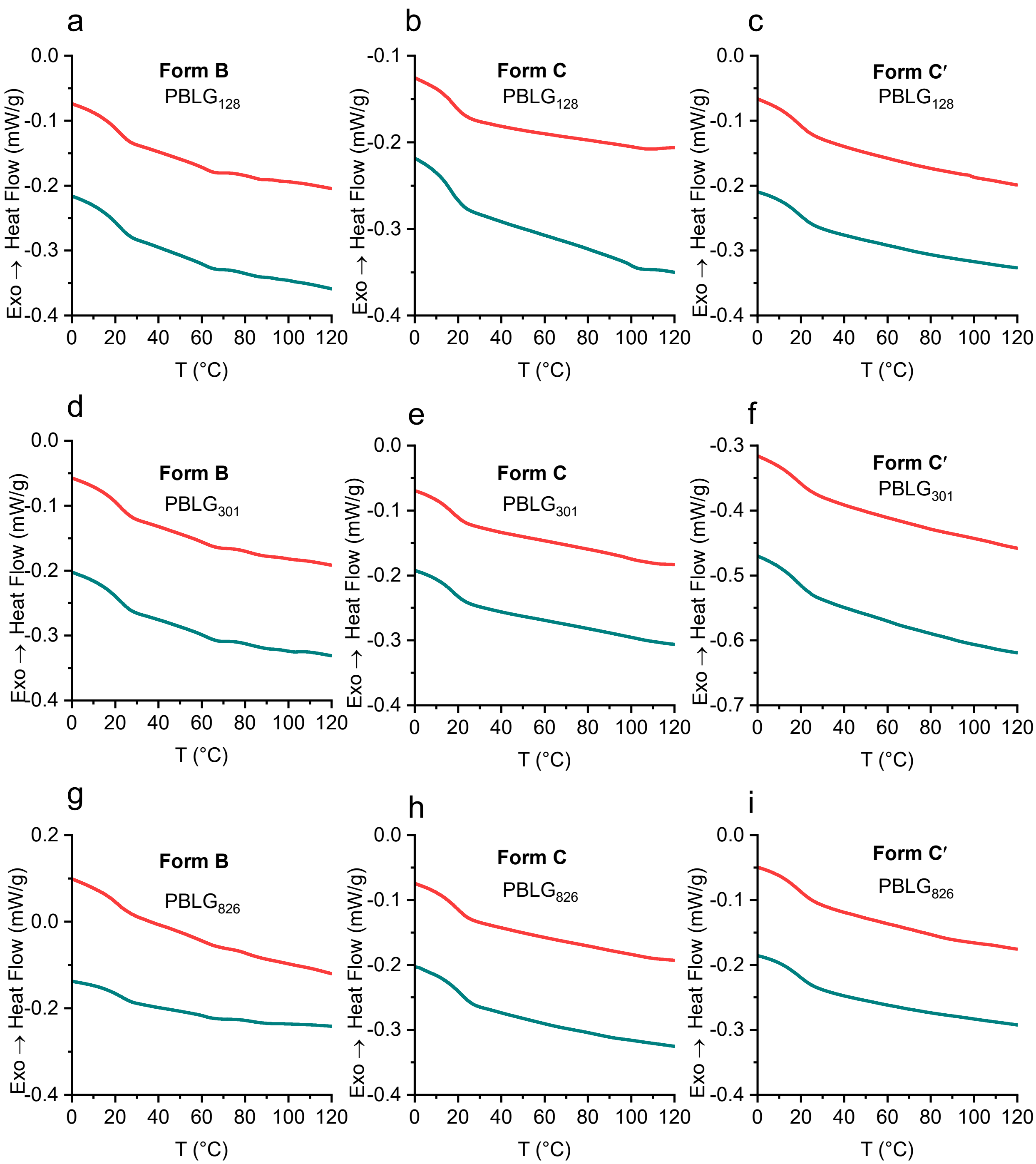

Figure S18. DSC curves on second heating for two replicates of films processed from linear PBLG. (a,d,g) Form B, (b,e,h) Form C, (c,f,i) Form C′. (a-c) $PBLG_{128}$, (d-f) $PBLG_{301}$, (g-i) $PBLG_{826}$.

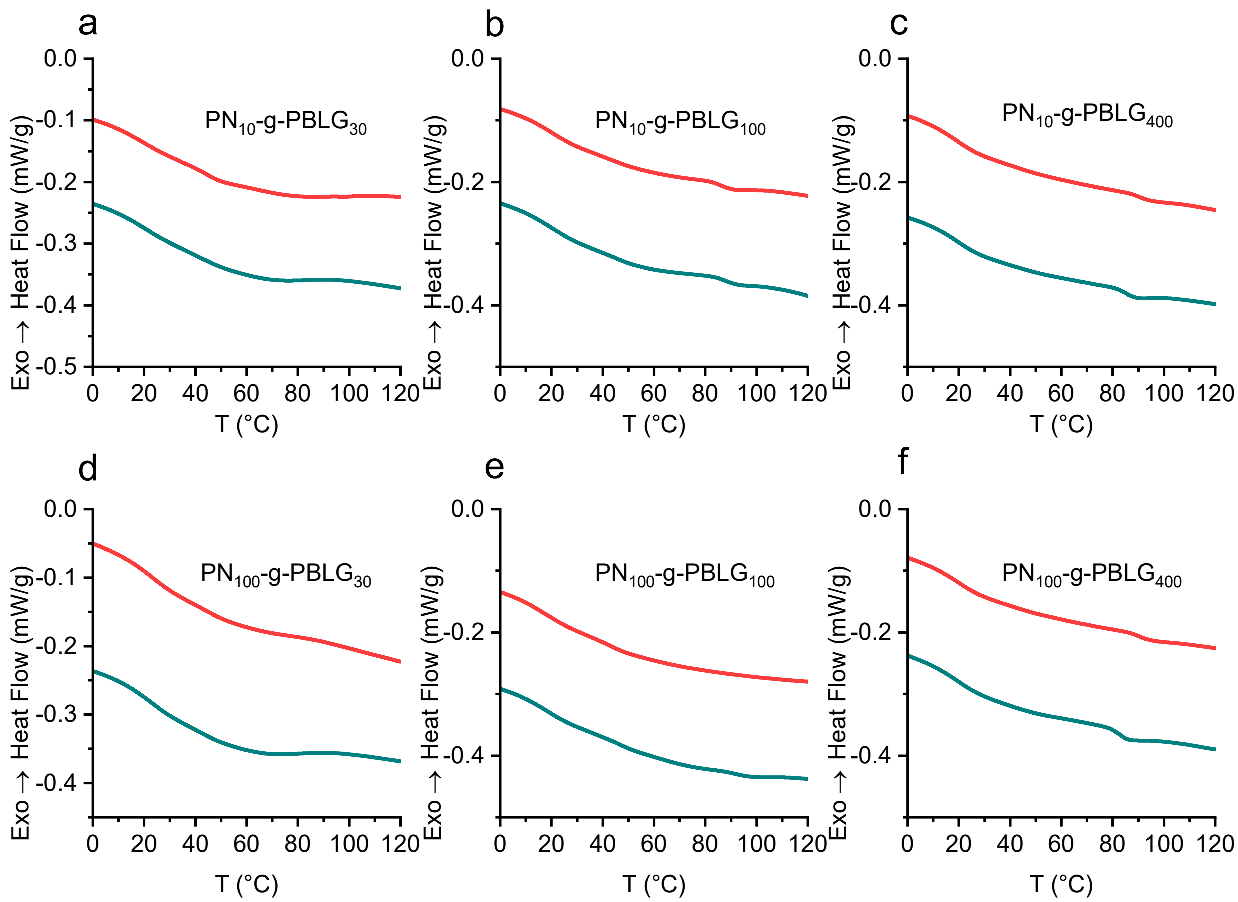

Figure S19. DSC curves on first heating for two replicates of hot processed films from comb-like and brush-like polymers. (a-c) Comb-like, (d-f) Brush-like.

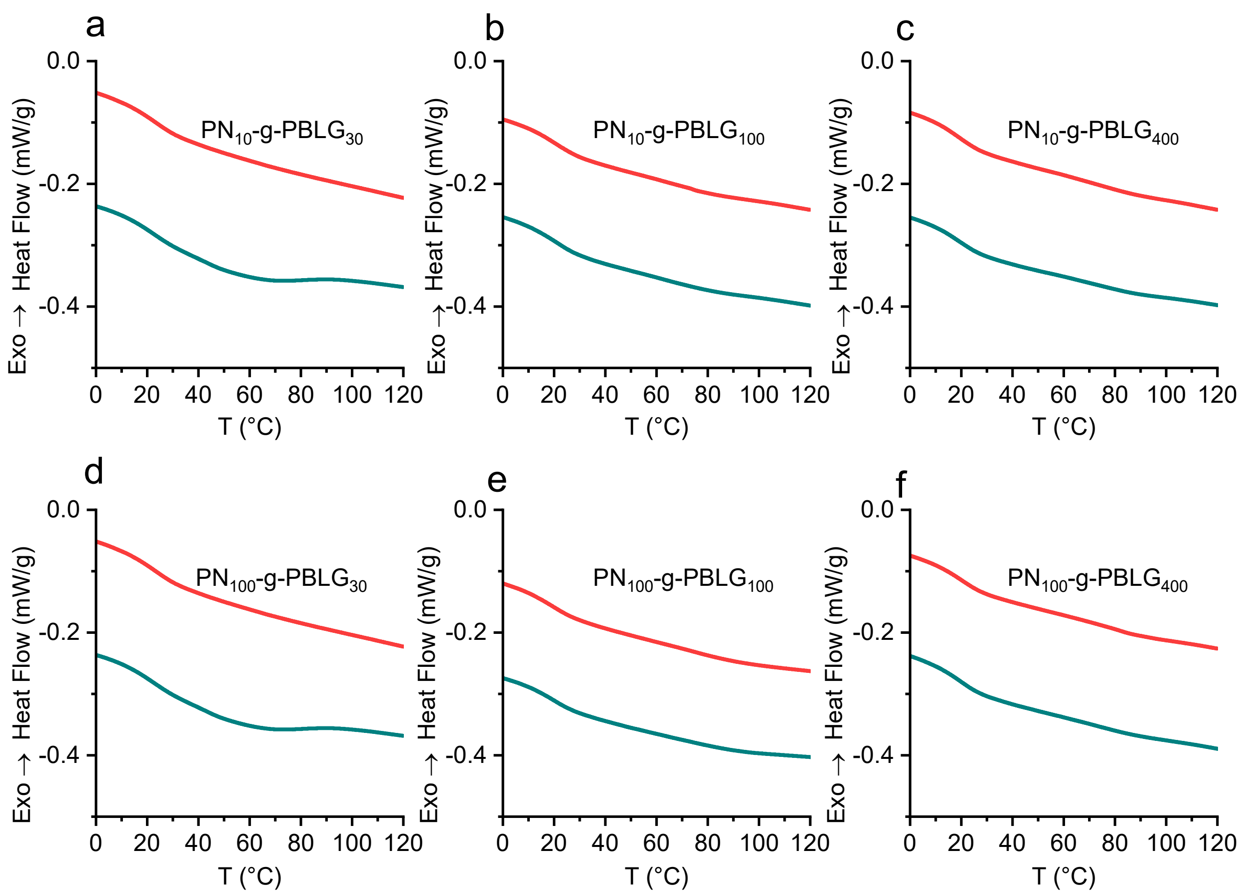

Figure S20. DSC curves on second heating for two replicates of hot processed films from comb-like and brush-like polymers. (a-c) Comb-like, (d-f) Brush-like.

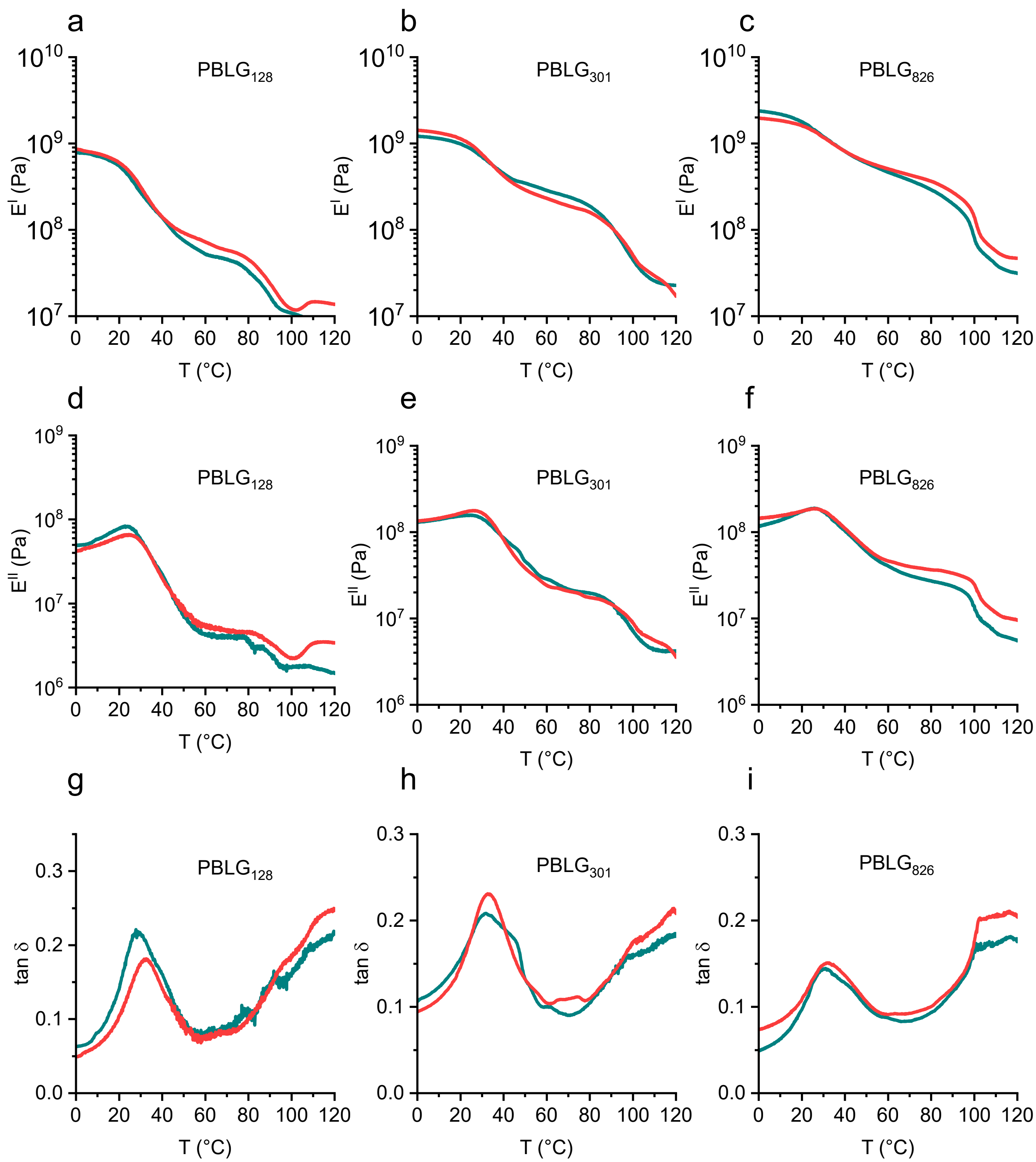

Figure S21. E', E'', and tan δ as a function of temperature for two replicates of cast films of Form B with three different chain lengths. (a-c) E', (d-f), E'', (g-i) tan δ. The three different chain lengths are $PBLG_{128}$ (a,d,g), $PBLG_{301}$ (b,e,h), and $PBLG_{826}$ (c,f,i). Cast films of $PBLG_{128}$ were fragile and tended to fracture during loading and running of the experiment.

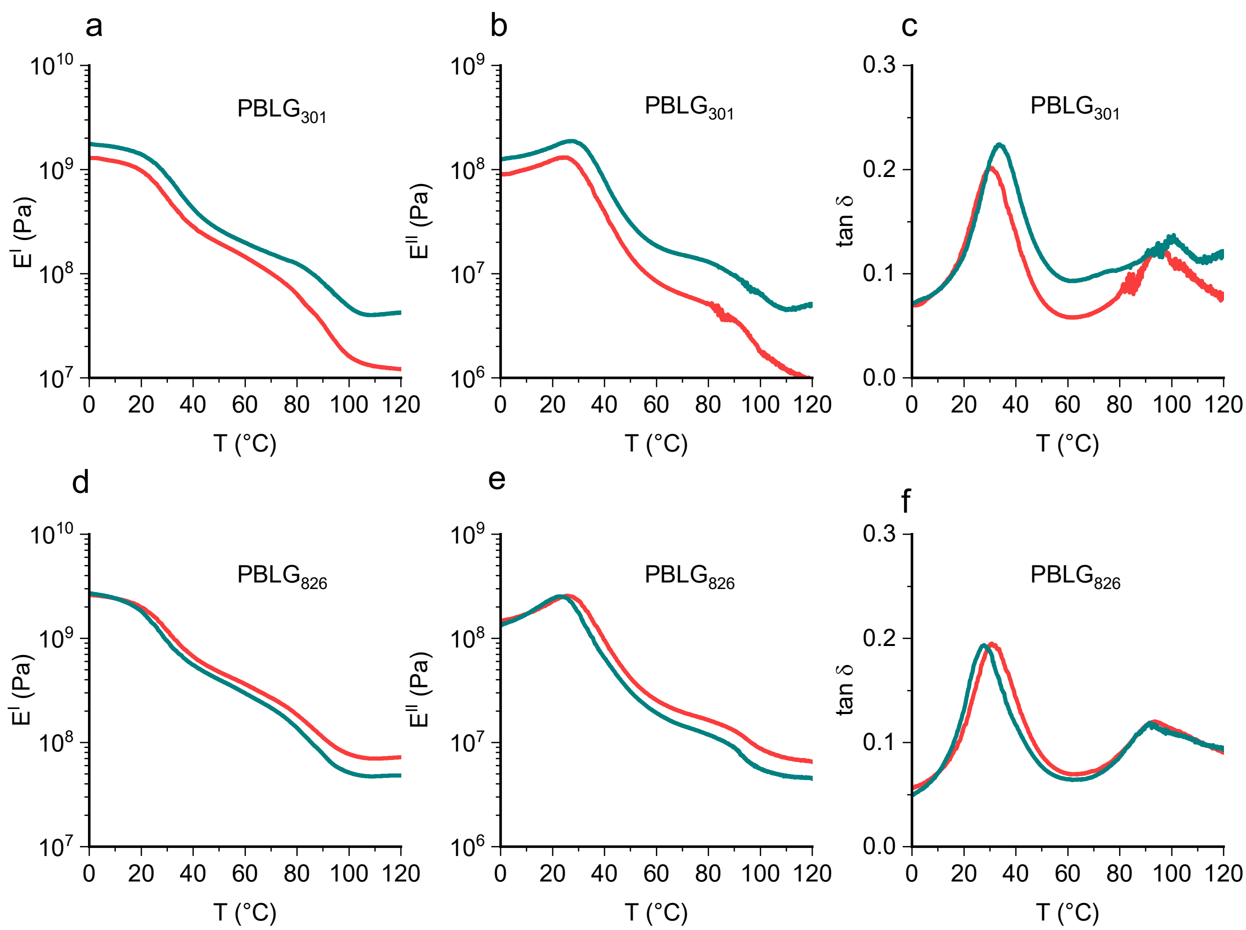

Figure S22. E', E'', and tan δ as a function of temperature on second heating for two replicates of cast films of Form B with two different chain lengths. (a,d) E', (b,e), E'', (c-f) tan δ. The two chain lengths are $PBLG_{301}$ (a-c), and $PBLG_{826}$ (d-f). A second heating was not possible for $PBLG_{128}$ cast films owing to their fragile nature.

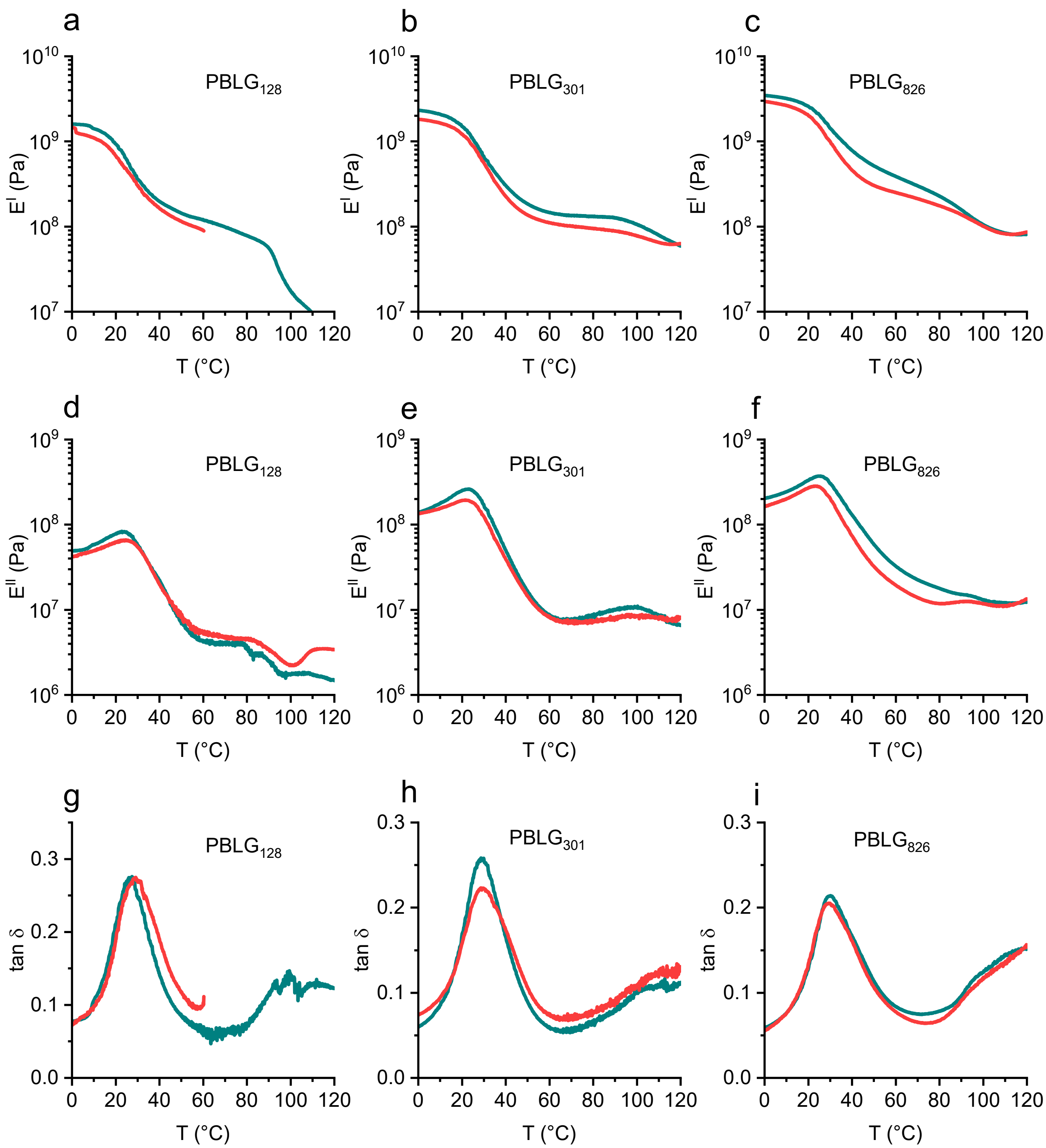

Figure S23. E', E'', and tan δ as a function of temperature for two replicates of cast films of Form C with three different chain lengths. (a-c) E', (d-f), E'', (g-i) tan δ. The three different chain lengths are $PBLG_{128}$ (a,d,g), $PBLG_{301}$ (b,e,h), and $PBLG_{826}$ (c,f,i). Cast films of $PBLG_{128}$ were fragile and tended to fracture during loading and running of the experiment.

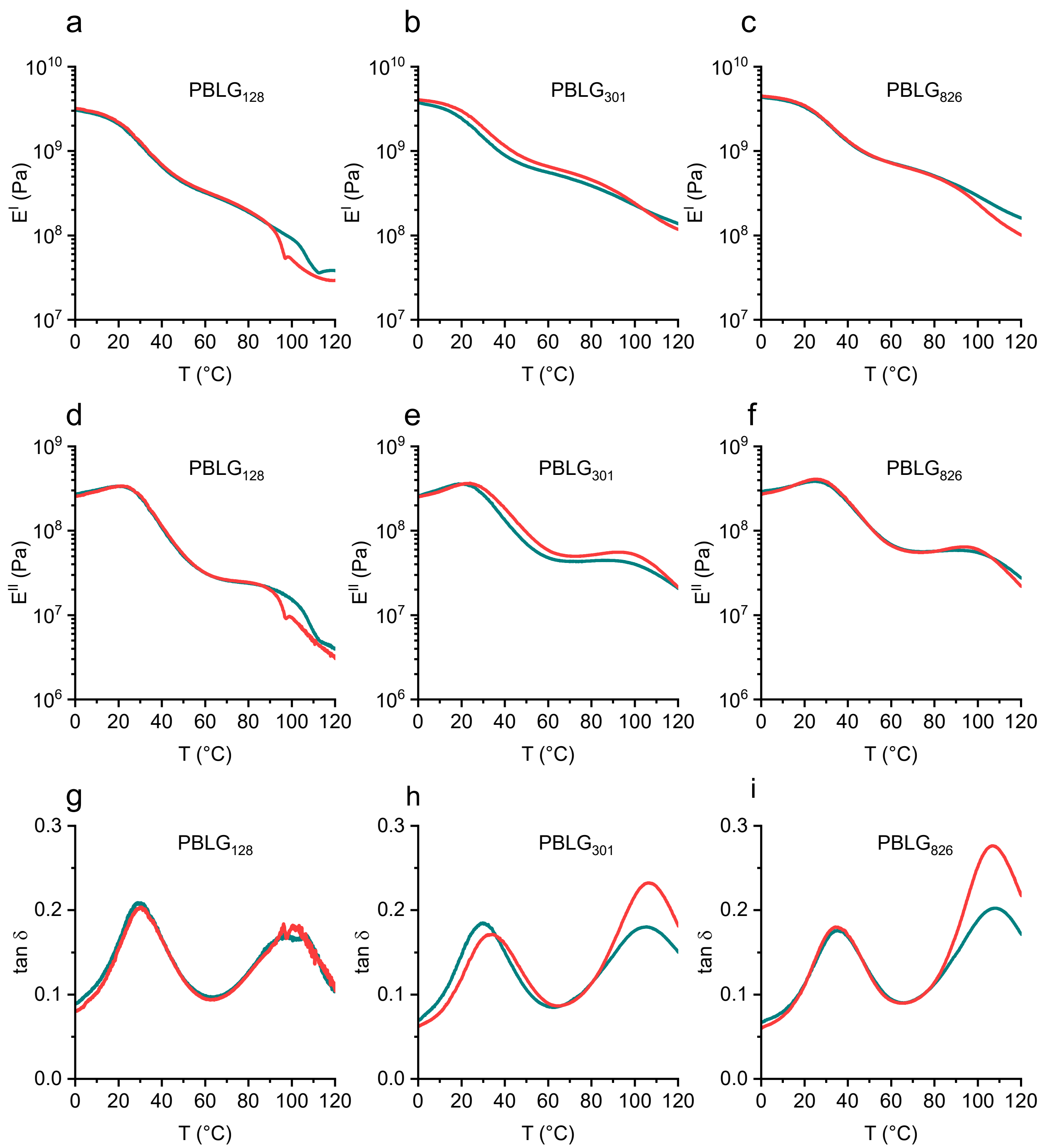

Figure S24. E', E'', and tan δ as a function of temperature for two replicates of cast films of Form C′ with three different chain lengths. (a-c) E', (d-f), E'', (g-i) tan δ. The three different chain lengths are $PBLG_{128}$ (a,d,g), $PBLG_{301}$ (b,e,h), and $PBLG_{826}$ (c,f,i).

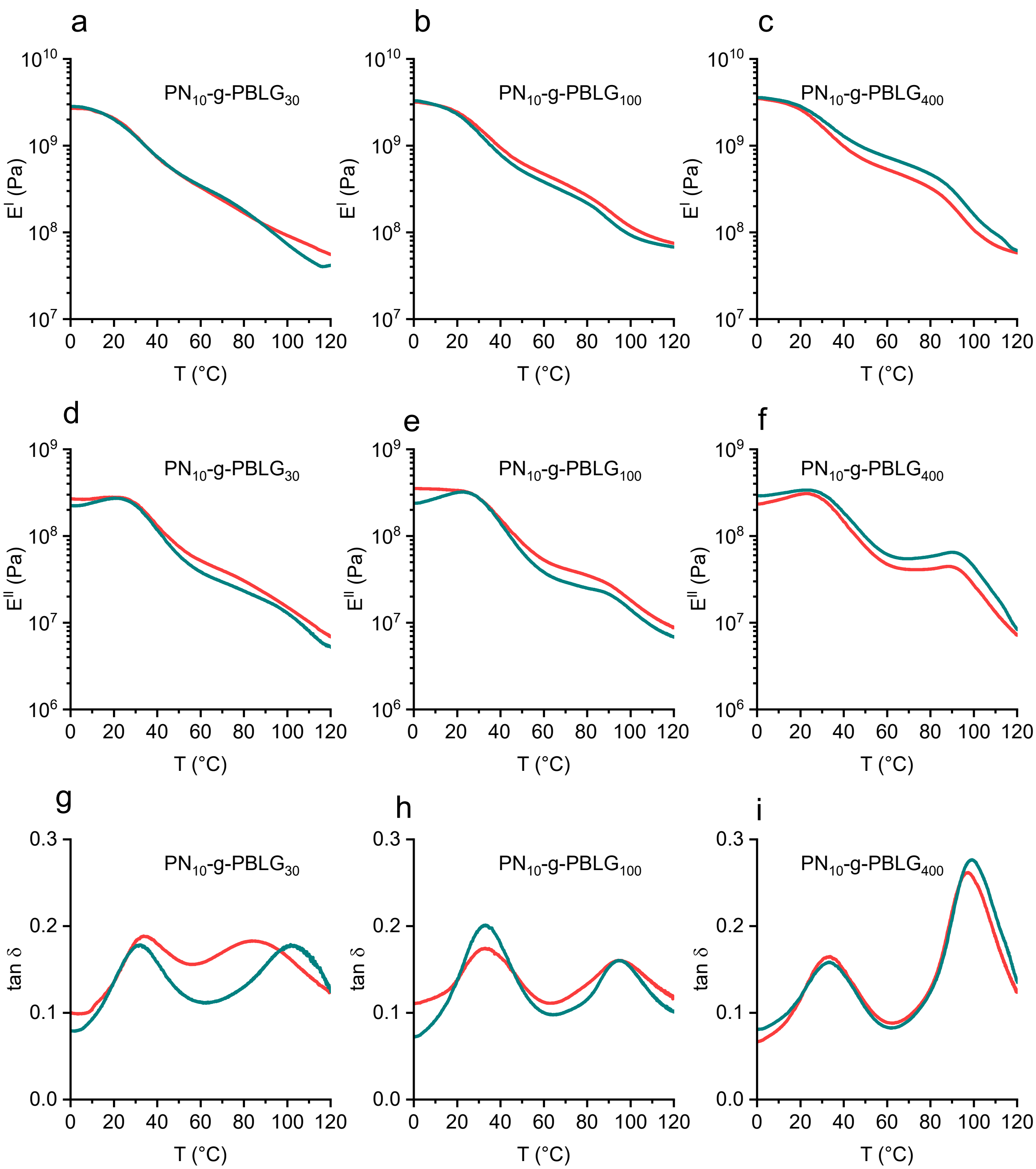

Figure S25. E', E'', and tan δ as a function of temperature for two replicates of hot pressed films of comb-like macromolecules with three different grafted PBLG chain lengths. (a-c) E', (d-f), E'', (g-i) tan δ. *g*-$PBLG_{30}$ (a,d,g), *g*-$PBLG_{100}$ (b,e,h), *g*-$PBLG_{400}$ (c,f,i). Films of $PBLG_{10}$-*g*-$PBLG_{30}$ were fragile and tended to fracture during loading and running of the experiment.

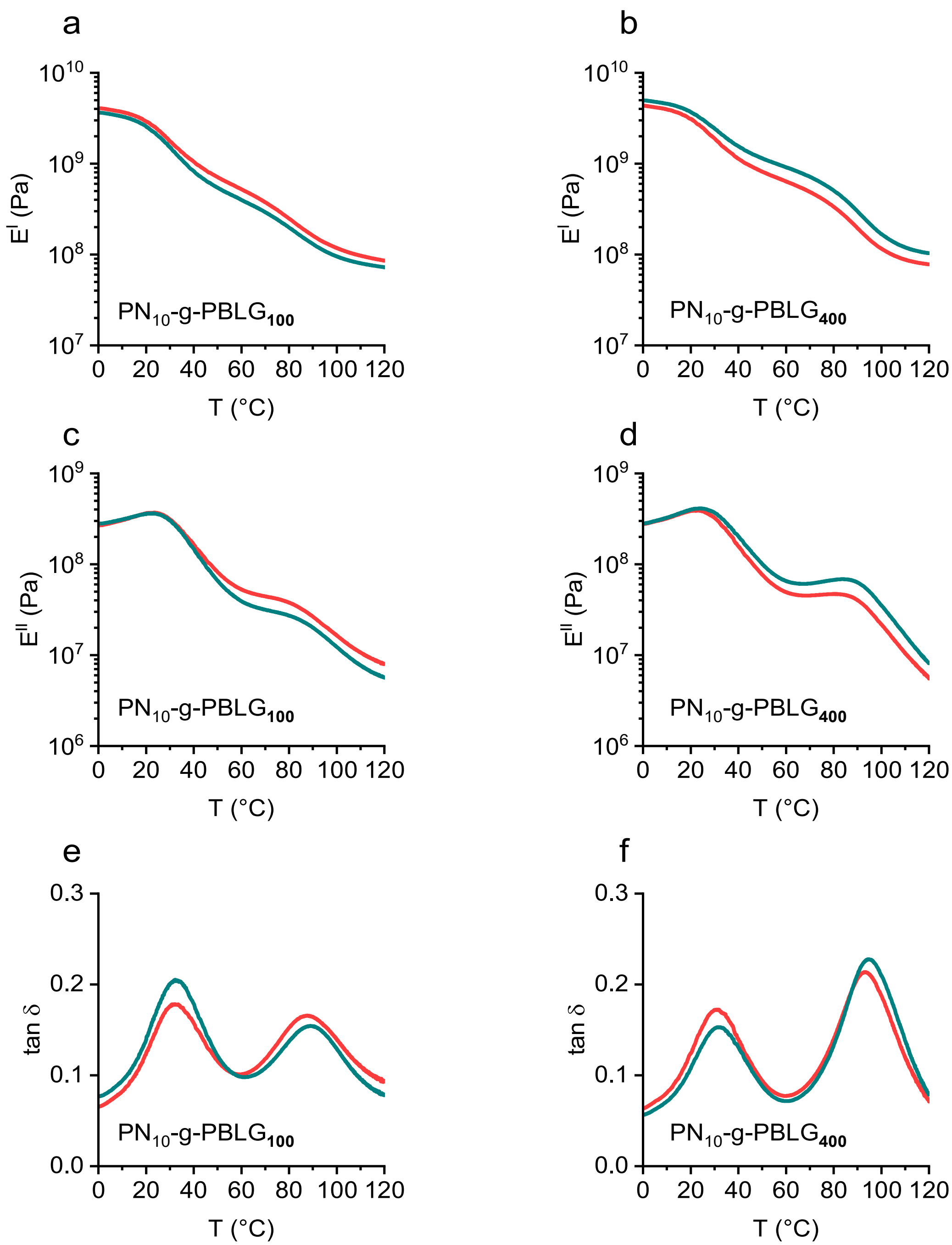

Figure S26. E', E'', and tan δ as a function of temperature on second heating for two replicates of hot pressed films of comb-like macromolecules with two different grafted PBLG chain lengths. (a,b) E', (c,d) E'', (e-f) tan δ. *g*-PBLG$_{100}$ (a,c,e), *g*-PBLG$_{400}$ (b,d,f). A second heating was not possible for PN$_{10}$-*g*-PBLG$_{30}$ owing to their fragile nature.

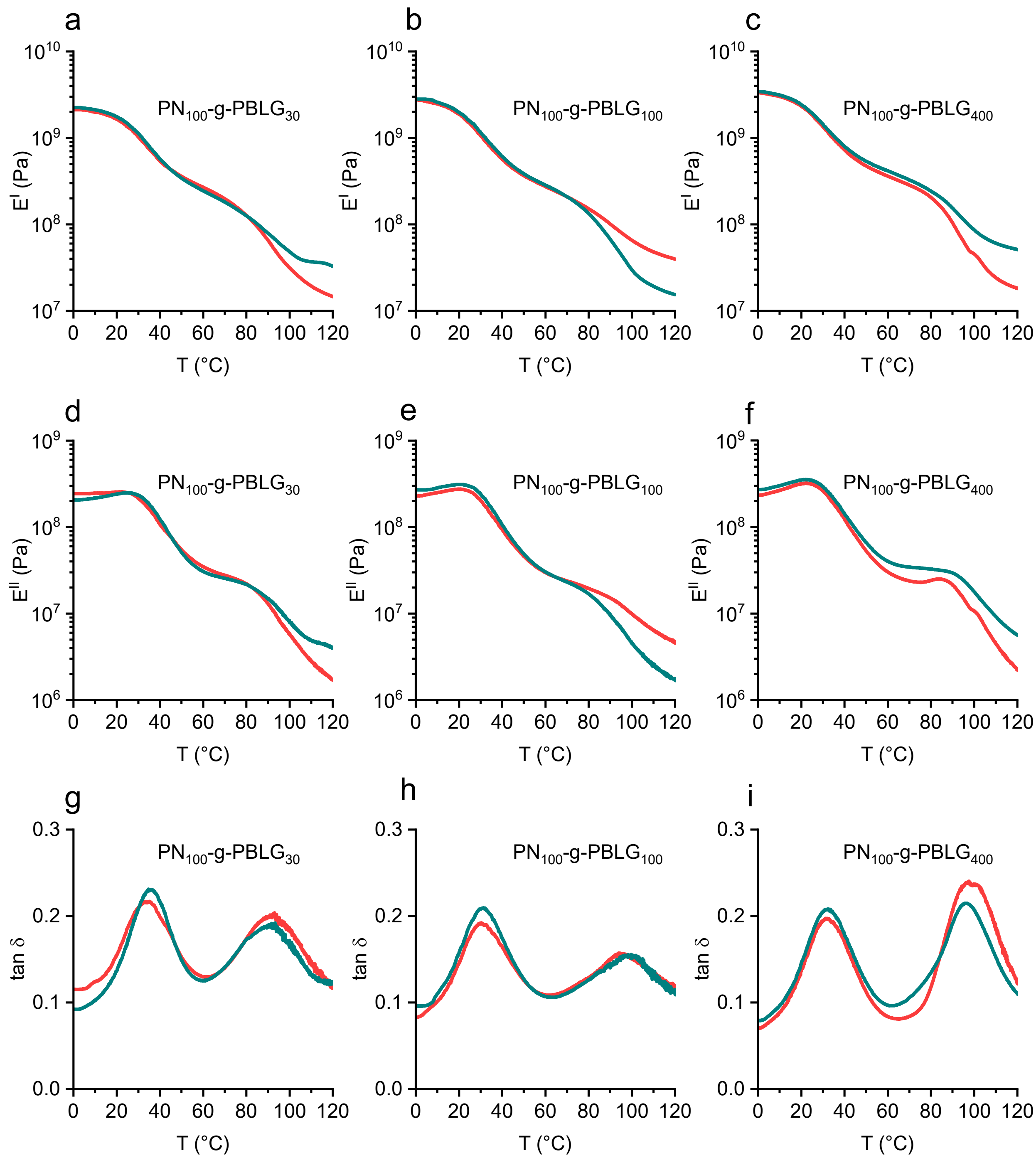

Figure S27. *E′*, *E″*, and tan *δ* as a function of temperature for two replicates of hot pressed films of brush-like macromolecules with three different grafted PBLG chain lengths. (a-c) *E′*, (d-f), *E″*, (g-i) tan *δ*. *g*-$PBLG_{30}$ (a,d,g), *g*-$PBLG_{100}$ (b,e,h), *g*-$PBLG_{400}$ (c,f,i). Films of $PBLG_{100}$-*g*-$PBLG_{30}$ were fragile and tended to fracture during loading and running of the experiment.

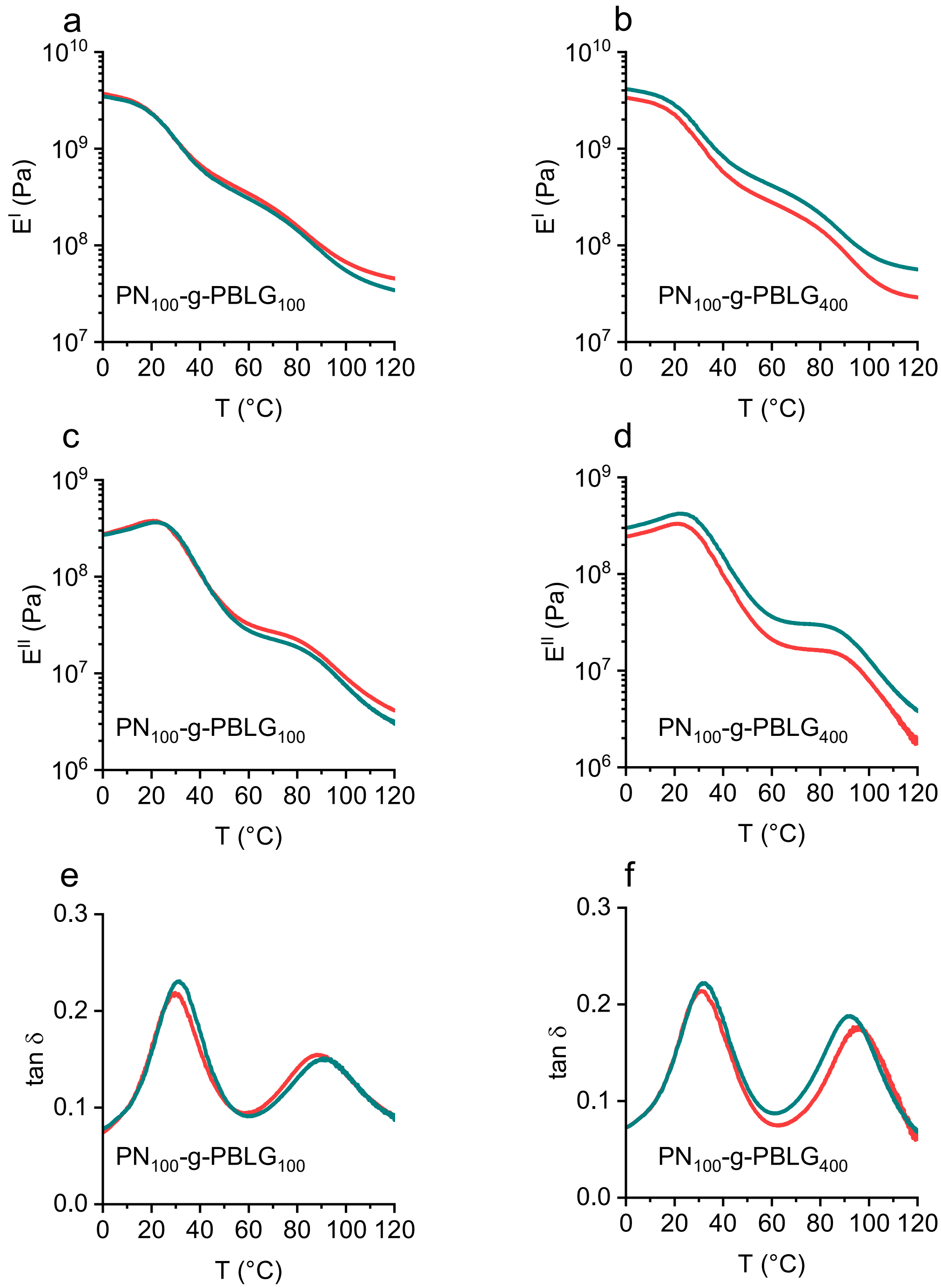

Figure S28. *E′*, *E″*, and tan *δ* as a function of temperature on second heating for two replicates of hot pressed films of brush-like macromolecules with two different grafted PBLG chain lengths. (a,b) *E′*, (c,d) *E″*, (e-f) tan *δ*. *g*-$PBLG_{100}$ (a,c,e), *g*-$PBLG_{400}$ (b,d,f). A second heating was not possible for PN_{100}-*g*-$PBLG_{30}$ owing to their fragile nature.

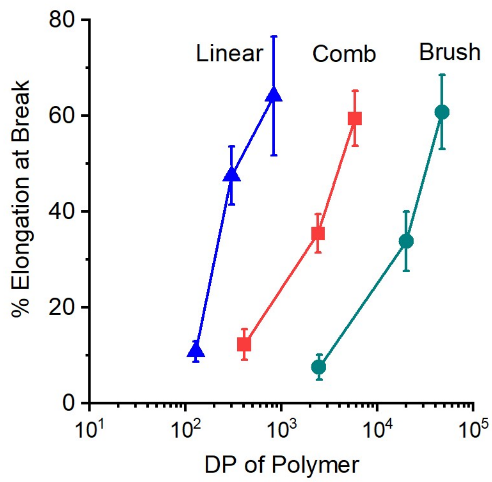

Figure S29. Summary of elongation at break values for the stress-strain behaviors of linear, comb-, and brush-like PBLGs at 40 °C.

Unit Cell Optimization

The d-spacings and unit cell for solution cast films were obtained using CLEARER software[1]. The diffraction settings used in CLEARER were obtained from XRD2DSCAN software[2].

1. Sumner Makin, O.; Sikorski, P.; Serpell, L. C. CLEARER : a new tool for the analysis of X-ray fibre diffraction patterns and diffraction simulation from atomic structural models. Journal of applied crystallography 2007, 40, 966-972.

2. Rodriguez-Navarro, A. B. XRD2DScan: new software for polycrystalline materials characterization using two-dimensional X-ray diffraction. Journal of Applied Crystallography 2006, 39, 905-909.

Table S1. X-Ray Spacings of Form C

Miller Indices			d-Spacings (Å)		
h	k	l	$PBLG_{128}$	$PBLG_{301}$	$PBLG_{826}$
1	0	0	12.98	12.78	vw
0	1	0	vw	vw	12.51
1	1	0	7.43	7.25	7.31
0	2	0	6.38	6.18	6.25
0	0	5	5.40	vw	vw
0	0	6	4.50	vw	vw
0	0	13	vw	2.07	2.07

[vw]Bragg's reflection is very weak

Table S2. Unit Cell Parameters for Form C showing reflections index on a hexagonal unit cell

Film	a (Å)	b (Å)	c (Å)	γ (°)
$PBLG_{128}$	15.0	14.7	27	120
$PBLG_{301}$	14.7	14.3	27	120
$PBLG_{826}$	14.8	14.4	27	120
Literature[a]	14.8 – 15.2	14.3 – 14.8	27	118 - 120

[a]Watanabe, J.; Imai, K.; Gehani, R.; Uematsu, I. Structural differences between two crystal modifications of poly(γ-benzyl L-glutamate). Journal of polymer science. 1981, 19, 653-665

Table S3. X-Ray Spacings of Form B

Miller Indices			d-Spacings (Å)		
h	k	l	$PBLG_{128}$	$PBLG_{301}$	$PBLG_{826}$
1	0	0	14.31	14.17	14.18
0	1	0	12.18	12.21	11.99
1	1	0	7.78	7.81	7.75
-1	2	0	6.73	6.68	6.54
1	2	0	4.90	vw	4.86
0	0	5	5.40	vw	vw
0	0	6	4.50	4.50	vw
0	0	7	vw	3.85	3.85
0	0	8	vw	vw	3.38
0	0	9	vw	vw	3.00

[vw]Bragg's reflection is very weak

Table S4. Unit Cell Parameters for Form B showing reflections index on a monoclinic unit cell

Film	a (Å)	b (Å)	c (Å)	γ (°)
$PBLG_{128}$	15.82	13.46	27	115.26
$PBLG_{301}$	15.52	13.37	27	113.99
$PBLG_{826}$	15.49	13.09	27	113.70
Literature[a]	15.88	13.00	27	113.70

[a]McKinnon, A. J.; Tobolsky, A. V. Structure and properties of poly(.gamma.-benzyl-L-glutamate) cast from dimethylformamide. *The journal of physical chemistry*. **1968**, *72*, 1157-1161.

Statistical Analysis Methodology for Stress-Strain Data

Linear regression analysis was performed using Minitab software to determine the statistical relationship between input variable (predictor) of chain length and output variables (response) of % elongation at break and strength at break; amongst different processing methods; between different macromolecular architecture, using a significance level (α) of 0.1. α is the probability of rejecting the null hypothesis (null hypothesis is no relationship) when it is true. The p-value, the probability of obtaining an effect at least as extreme as the one in your sample data if the null hypothesis is assumed to be true, was used as a measure of statistical significance. If the p-value of the predictor in the test of significance is lower than or equal to the significance level, then the null hypothesis can be rejected, and the results are statistically significant. This implies that the changes in the predictor's value are related to changes in the response variable. P-values that are larger than the significance level indicate that the results are not statistically significant. In this case, the changes in the predictor are not related to changes in the response variable.

Determining the significance of chain length

Linear regression was performed on form B, form C, form C′, and comb-like and brush-like stress-strain data. The chain length of the linear PBLG films and the DP of PBLG for the comb-like and brush-like films were used as predictors. Therefore, the p-value of chain length and DP of PBLG determine the significance. Statistical significance occurs when p-value is ≤ 0.1 while insignificance occurs when $p > 0.1$.

Comparing processing methods and molecular architecture

The regression lines for form B, form C and form C′ were compared to determine whether their constants and slope coefficients are different. To compare the constants, a categorical variable (condition C for form C, condition C′ for form C′) was included in the linear regression analysis. This categorical variable represents the vertical shift in the y intercept. The interaction between chain length and the categorical variable (chain length*condition) is a measure of whether the effect of chain length depends on the condition. The p-value of this interaction term determines significance of the difference between slopes. A similar treatment was performed on the comb-like and brush-like polymers with the categorical variable being condition C for comb-like architecture and the interaction term being DP of PBLG*condition C.

Linear PBLG Results

Table S5. Linear Regression Coefficients for % Elongation at Break for Stress-Strain at 0 °C for Form B and Form C to determine significance of chain length using the p-value of chain length

Output	Form B		Form C	
	Term		Term	
	Y intercept	Chain Length	Y intercept	Chain Length
Coef	0.606	0.007	0.459	0.036
SE Coef	0.184	0.001	0.453	0.004
T-Value	3.290	4.500	1.010	8.960
P-Value	0.030	0.011[a]	0.369	0.001[a]

[a]P-value indicates that chain length is significant

Table S6. Linear Regression Coefficients of % Elongation at Break for Stress-Strain at 0 °C for a comparison of the y intercept and slope of Regression Lines of Form B and Form C using the p-value of Condition C and Chain Length*Condition C

Term	Coef	SE Coef	T-Value	P-Value
Constant	0.606	0.346	1.750	0.118
Chain Length	0.007	0.003	2.400	0.043
Condition C	-0.147	0.489	-0.300	0.771[a]
Chain Length*Condition C	0.029	0.004	6.600	< 0.001[b]

[a]P-value indicates that the difference between y intercepts of form B and C is not statistically significant

[b]P-value indicates that difference between slopes of form B and C is statistically significant

Table S7. Linear Regression Coefficients for Strength at Break for Stress-Strain at 0 °C for Form B and Form C to determine significance of chain length using the p-value of chain length

Output	Form B Term		Form C Term	
	Y intercept	Chain Length	Y intercept	Chain Length
Coef	4.470	0.017	-2.270	0.219
SE Coef	0.924	0.008	2.420	0.022
T-Value	4.840	2.070	-0.940	10.200
P-Value	0.008	0.107[a]	0.401	0.001[a]

[a]P-value indicates that chain length is significant

Table S8. Linear Regression Coefficients of Strength at Break for Stress-Strain at 0 °C for a comparison of the y intercept and slope of Regression Lines of Form B and Form C using the p-value of Condition C and Chain Length*Condition C

Term	Coef	SE Coef	T-Value	P-Value
Constant	4.47	1.830	2.440	0.040
Chain Length	0.017	0.016	1.040	0.327
Condition C	-6.740	2.590	-2.600	0.031[a]
Chain Length*Condition C	0.202	0.023	8.790	< 0.001[b]

[a]P-value indicates that the difference between y intercepts of form B and C is statistically significant

[b]P-value indicates that difference between slopes of form B and C is statistically significant

Table S9. Linear Regression Coefficients for % Elongation at Break for Stress-Strain at 40 °C for Form B, Form C and Form C′ to determine significance of chain length using the p-value of chain length

Output	Form B		Form C		Form C′	
	Term		Term		Term	
	Y intercept	Chain Length	Y intercept	Chain Length	Y intercept	Chain Length
Coef	0.010	0.176	7.980	0.119	13.230	0.301
SE Coef	2.840	0.025	4.240	0.038	9.470	0.084
T-Value	< 0.001	7.010	1.880	3.170	1.400	3.570
P-Value	0.998	0.002[a]	0.133	0.034[a]	0.235	0.023[a]

[a]P-value indicates that chain length is significant

Table S10. Linear Regression Coefficients of % Elongation at Break for Stress-Strain at 40 °C for a comparison of the y intercept and slope of Regression Lines of Form B, Form C and Form C′ and Form C using the p-value of Condition C, Condition C′, Chain Length*Condition C and Chain Length*Condition C′

Term	Coef	SE Coef	T-Value	P-Value
Constant	0.010	6.210	< 0.001	0.999
Chain Length	0.176	0.055	3.190	0.008
Condition C	7.970	8.780	0.910	0.382[a]
Condition C'	13.220	8.780	1.510	0.158[b]
Chain Length*Condition C	-0.056	0.078	-0.720	0.485[c]
Chain Length*Condition C'	0.125	0.078	1.600	0.135[d]

[a,b]P-value indicates that y intercept of form C and form C′ are not significantly different from form B

[c,d]P-value indicates that slope of form C and form C′ are not significantly different from form B

Table S11. Linear Regression Coefficients for Strength at Break for Stress-Strain at 40 °C for Form B, Form C and Form C′ to determine significance of chain length using the p-value of chain length

Term	Form B		Form C		Form C′	
	Term		Term		Term	
	Y intercept	Chain Length	Y intercept	Chain Length	Y intercept	Chain Length
Coef	0.923	0.028	1.491	0.056	4.550	0.085
SE Coef	0.634	0.005	0.573	0.005	0.657	0.006
T-Value	1.460	4.940	2.600	11.050	6.920	14.560
P-Value	0.219	0.008[a]	0.060	< 0.001[a]	0.002	< 0.001[a]

[a]P-value indicates that chain length is significant

Table S12. Linear Regression Coefficients of Strength at Break for Stress-Strain at 40 °C for a comparison of the y intercept and slope of Regression Lines of Form B, Form C and Form C′ using the p-value of Condition C, Condition C′, Chain Length*Condition C and Chain Length*Condition C′

Term	Coef	SE Coef	T-Value	P-Value
Constant	0.923	0.623	1.480	0.164
Chain Length	0.028	0.005	5.030	< 0.001
Condition C	0.567	0.880	0.640	0.531[a]
Condition C'	3.626	0.880	4.120	0.001[b]
Chain Length*Condition C	0.029	0.007	3.640	0.003[c]
Chain Length*Condition C'	0.057	0.007	7.310	0.000[d]

[a,b]P-value indicates that y intercept of form C is not significantly different from form B but y intercept of form C′ is statistically significantly different from form B

[c,d]P-value indicates that slope of form C and form C′ are statistically significantly different from form B

Comb-like and Brush-like Polymer Results

Table S13. Linear Regression Coefficients for % Elongation at Break for Stress-Strain at 40 °C for comb-like and brush-like polymers to determine significance of PBLG chain length using the p-value of DP of PBLG

Output	Comb-like Term		Brush-like Term	
	Y intercept	DP of PBLG	Y intercept	DP of PBLG
Coef	15.730	0.113	11.460	0.128
SE Coef	4.900	0.021	5.800	0.024
T-Value	3.210	5.520	1.980	5.270
P-Value	5.520	0.005[a]	0.119	0.006[a]

[a]P-value indicates that DP of PBLG is significant

Table S14. Linear Regression Coefficients of % Elongation at Break for Stress-Strain at 40 °C for a comparison of the y intercept and slope of Regression Lines of comb-like and brush-like architectures using the p-value of Condition C and DP of PBLG*Condition C

Term	Coef	SE Coef	T-Value	P-Value
Constant	11.460	5.370	2.130	0.065
DP of PBLG	0.128	0.023	5.690	< 0.001
Condition C	4.270	7.590	0.560	0.589[a]
DP of PBLG*Condition C	-0.015	0.032	-0.460	0.656[b]

[a,b]P-value indicates that the y intercept and slope of the comb-like and brush-like architectures are not statistically significantly different

Table S15. Linear Regression Coefficients for Strength at Break for Stress-Strain at 40 °C for comb-like and brush-like polymers to determine significance of PBLG chain length using the p-value of DP of PBLG

Output	Comb-like		Brush-like	
	Term		Term	
	Y intercept	DP of PBLG	Y intercept	DP of PBLG
Coef	7.799	0.011	7.120	0.008
SE Coef	0.448	0.002	1.110	0.005
T-Value	17.400	5.78	6.400	1.870
P-Value	< 0.001	0.004[a]	0.003	0.135[b]

[a,b]P-value indicates that DP of PBLG is significant in the comb-like architecture but not significant in the brush-like architecture

Table S16. Linear Regression Coefficients of Strength at Break for Stress-Strain at 40 °C for a comparison of the y intercept and slope of Regression Lines of comb-like and brush-like architectures using the p-value of Condition C and DP of PBLG*Condition C

Term	Coef	SE Coef	T-Value	P-Value
Constant	7.118	0.848	8.390	< 0.001
DP of PBLG	0.009	0.004	2.450	0.040
Condition C	0.680	1.200	0.570	0.585[a]
DP of PBLG*Condition C	0.002	0.005	0.430	0.681[b]

[a,b]P-value indicates that the y intercept and slope of the comb-like and brush-like architectures are not statistically significantly different